Anomalous reflection in a metallic plate with subwavelength grooves of circular cross section

Claudio I. Valencia[1] and Diana C. Skigin[2,*]

[1]Facultad de Ciencias, Universidad Autónoma de Baja California, Km. 107 Carretera Tijuana-Ensenada, Ensenada, Baja California 22860, Mexico; vale@uabc.mx

[2]Grupo de Electromagnetismo Aplicado, Departamento de Física, Facultad de Ciencias Exactas y Naturales, Universidad de Buenos Aires, Ciudad Universitaria, Pabellón I, C1428EHA Buenos Aires, Argentina; also member of CONICET

*Corresponding author: dcs@df.uba.ar

Received 15 July 2009; accepted 2 September 2009;
posted 1 October 2009 (Doc. ID 114316); published 19 October 2009

Resonant features in the response of finite arrays of rectangular grooves ruled on a metallic plate have been reported in connection with the excitation of phase resonances. These anomalies are generated by a particular arrangement of the magnetic field phases inside the subwavelength grooves when the structure is illuminated by a *p*-polarized electromagnetic wave. We show that this kind of resonance is also present for grooves of circular cross section and appear as sharp peaks in the specular response, the number of which increases with the number of grooves in the structure. A significant intensification of the field within the grooves is also found for these particular phase configurations. The dependence of the response on the geometrical parameters of the structure is analyzed in detail, in order to consider these structures for potential applications such as frequency selectors and polarizers. © 2009 Optical Society of America

OCIS codes: 050.1950, 240.3695.

1. Introduction

Recent progress in fabrication techniques has increased the interest of the scientific community in studying structures with subwavelength slits due to their interesting properties and multiple applications. For instance, nanowire gratings have been proposed for the characterization of attosecond pulses [1], integrated polarizers [2], optical data storage, and external storage media.

Gratings with subwavelength slits or grooves have also attracted much theoretical interest due to their capability to produce unusual phenomena such as enhanced transmission [3–6]. The excitation of phase resonances in such systems also produces unexpected responses, and this phenomenon has also been investigated in the past few years [7–19]. A decade ago Veremey and Mittra demonstrated that the scattered field of a structure formed by a finite number of slotted cylinders exhibits superdirective characteristics at the resonant frequencies of the system [20]. The occurrence of superdirectivity is attributed to the excitation of modes that induce a phase reversal in the adjacent scatterers (phase resonances). Later on, this property was also found in structures formed by a finite array of rectangular grooves on a metallic plane [7], suggesting that this property is a common attribute of systems formed by coupled resonant elements. The excitation of phase resonances in such a system appears as sharp peaks in the reflected response and is accompanied by a significant enhancement of the field within the grooves. Recently, the investigation of phase resonances has also

0003-6935/09/305863-08$15.00/0

been extended to infinitely periodic reflection gratings [8–10,18] and transmission wire gratings [12–17,19], where interesting properties have been demonstrated. It is important to note that all the research done on the excitation of phase resonances on surfaces considered grooves of rectangular geometry.

In this paper we investigate the electromagnetic response of a system formed by a finite number of subwavelength grooves of circular cross section on a perfectly conducting plate, paying particular attention to the excitation of phase resonances on the structure. To solve the scattering problem, we use an integral method [21–23]. An improvement of the method has been done to deal with sharp corners of the structure, as those appearing in the system studied. This method is very versatile and convenient, especially to deal with arbitrary shapes of the grooves.

In Section 2 we pose the scattering problem and outline the integral method applied to structures invariant along a certain direction, which is the case of the present system. The results obtained are shown in Section 3, where we display curves of reflected response as a function of the incident wavelength for normal and oblique incidence. We also study the dependence of the resonance on the relevant geometrical parameters of the structure such as the radius and the aperture. The behavior of the amplitude and phase of the field within the grooves at resonance is also investigated. Finally, the conclusions are summarized in Section 4.

2. Integral Method

Let us consider N cavity-like grooves of radius R, ruled on a perfectly conducting flat surface, as shown in Fig. 1. Since the structure and the field parameters are invariant along the z direction, the problem can be reduced to a two-dimensional one. Figures 1(a) and 1(b) show the outline corresponding to odd and even numbers of cavities, respectively. The even configuration of Fig. 1(b) also allows us to explore the response of two identical subsystems of $N/2$ cavities as a function of the distance $d+\Delta$ between them. This configuration is of interest as shown in the following section.

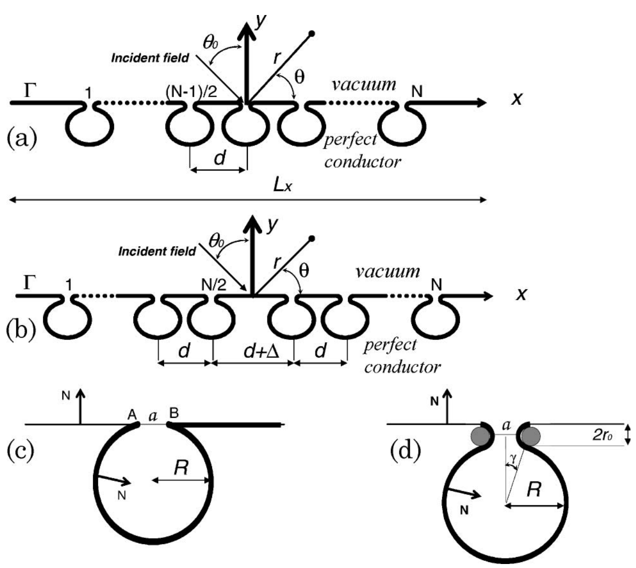

Fig. 1. Configuration of the scattering problem by a finite structure with grooves of circular cross section.

As it is well known, the integral method might exhibit numerical instabilities when the curve describing the profile presents abrupt changes. Different strategies have been proposed to deal with the singularities that arise in the corners [24]. In our approach, to overcome this difficulty, the sharp corners of the structure [points A and B in Fig. 1(c)] have been replaced by small arcs of radius r_0, as shown in Fig. 1(d) (the presence of the gray circles in the figure is just to emphasize this construction). The width of each aperture a is controlled by the angle γ and the radius r_0, according to the relation $a = 2[(r_0 + R)\sin\gamma - r_0]$.

We consider an incident field, impinging from vacuum on the perfectly conducting structure, independent of the z coordinate. Under this assumption, the magnetic field for a p-polarized radiation can be written as

$$\mathbf{H}(\mathbf{r}) = [\psi_{\mathrm{inc}}(\mathbf{r}) + \psi_{\mathrm{sc}}(\mathbf{r})]\hat{\mathbf{z}}, \tag{1}$$

where ψ_{inc} and ψ_{sc} are the complex amplitudes of the incident and scattered fields, respectively. The incident field can be written in terms of its angular spectrum $A(\alpha|\alpha_0)$ as

$$\psi_{\mathrm{inc}}(\mathbf{r}) = \frac{1}{2\pi}\int_{-\omega/c}^{\omega/c} A(\alpha|\alpha_0)\exp[i(\alpha x - \beta y)]\mathrm{d}\alpha, \tag{2}$$

where $\alpha_0 = (2\pi/\lambda)\sin\theta_0$, λ is the incident wavelength, and θ_0 is the angle of incidence. The propagation parameters α and β fulfill the condition $\beta = \sqrt{(2\pi/\lambda)^2 - \alpha^2}$, with $\mathrm{Re}(\alpha) > 0$ and $\mathrm{Im}(\beta) > 0$. In this paper, we assume a Gaussian distribution of the angular spectrum:

$$A(\alpha|\alpha_0) = \frac{\psi_0}{\sqrt{2\pi}\sigma}\exp[-(\alpha - \alpha_0)^2/(2\sigma^2)], \tag{3}$$

where σ is the angular dispersion of the beam and ψ_0 is a constant with the same units as the incident field.

The surface profile is represented by a vector-valued function $\mathbf{r}_s$, given by

$$\mathbf{r}_s = [\xi(t), \eta(t)], \tag{4}$$

where $\xi(t)$ and $\eta(t)$ are functions of the parameter t. For perfectly conducting materials and p-polarized waves, the integral equation can be written as

$$\psi(\mathbf{r}) = \psi_{\mathrm{inc}}(\mathbf{r}) + \frac{1}{4\pi}\int_\Gamma \frac{\partial G[\mathbf{r}|\mathbf{r}']}{\partial \mathbf{N}}\bigg|_{\mathbf{r}'=\mathbf{r}_s(t')} \times\psi(\mathbf{r}_s)\mathrm{d}l, \tag{5}$$

where ψ is the complex amplitude of the magnetic field, $\mathbf{N} = -(\mathrm{d}\eta/\mathrm{d}t)\hat{\mathbf{x}} + (\mathrm{d}\xi/\mathrm{d}t)\hat{\mathbf{y}}$ is a vector normal to the surface [see Fig. 1(c)], and $\mathrm{d}l$ is a differential of arc on the profile Γ. The Green function G in the kernel of the integral can be expressed in terms of the Hankel function of the first kind and order zero: $G(\mathbf{r}|\mathbf{r}') = i\pi H_0^{(1)}[(2\pi/\lambda)|\mathbf{r}-\mathbf{r}'|]$. To obtain the source functions $\psi(\mathbf{r}_s)$ from Eq. (5), it is assumed that the observation point $\mathbf{r}$ is on the profile Γ:

$$\psi(t) = \psi(t)_{\mathrm{inc}} + \frac{1}{4\pi}\lim_{\tau\to 0}\int_\Gamma \left.\frac{\partial G[\mathbf{r}_s^+|\mathbf{r}']}{\partial \mathbf{N}}\right|_{\mathbf{r}'=\mathbf{r}_s(t')} \times \psi(t')\mathrm{d}t', \tag{6}$$

where $\mathbf{r}_s^+ = \mathbf{r}_s(t) + \tau\mathbf{N}$. Once the source functions have been determined, ψ_{sc} can be evaluated as

$$\psi_{\mathrm{sc}}(\mathbf{r}) = \frac{i}{4}\int_\Gamma (2\pi/\lambda)\mathbf{N}\cdot\hat{\mathbf{u}}(t)H_1^{(1)}[(2\pi/\lambda)|\mathbf{u}(t)|]\times\psi(t)\mathrm{d}t, \tag{7}$$

$$H_{mn} = \begin{cases} \frac{i\pi\Delta t_n}{2\lambda}\{-\eta_n' u_{mn} + \xi_n' w_{mn}\}\frac{H_1^{(1)}\left(\frac{2\pi}{\lambda}\{u_{mn}^2+w_{mn}^2\}^{1/2}\right)}{\{u_{mn}^2+w_{mn}^2\}^{1/2}}, & m \neq n, \\ \frac{1}{2} + \frac{\Delta t_m}{4\pi\phi^2(t_m)}[\xi_m'\eta_m'' - \xi_m''\eta_m'], & m = n, \end{cases} \tag{13}$$

where $\mathbf{u}(t) = \mathbf{r} - \mathbf{r}_s(t)$, and $H_1^{(1)}$ is the Hankel function of the first kind and order one. At this stage, it is convenient to express the observation point $\mathbf{r}$ in polar coordinates r and θ. With this in mind, we can write Eq. (7) in terms of outgoing waves as

$$\psi_{\mathrm{sc}}(r,\theta) = \exp(i\pi/4)\frac{\exp[i(2\pi/\lambda)r]}{[16\pi^2 r/\lambda]^{1/2}}R(\theta), \tag{8}$$

where the scattering amplitude is

$$\begin{aligned} R(\theta) = i\int_\Gamma &(2\pi/\lambda)[\eta'(t')\cos\theta \\ &- \xi'(t')\sin\theta]\psi(t')\exp\{-i(2\pi/\lambda)[\xi(t')\cos\theta \\ &+ \eta(t')\sin\theta]\}\mathrm{d}t'. \end{aligned} \tag{9}$$

In writing Eq. (8) we have used the expansion of Hankel functions for large arguments [25] and the approximation $|\mathbf{u}| \approx r - (\xi(t)\cos(\theta) + \eta(t)\sin\theta)$ for the argument of the exponential.

The radial component of the time-averaged Poynting vector can be written as

$$\begin{aligned} (\mathbf{S}_{\mathrm{sc}})_r &= (c/(8\pi)\Re[\mathbf{E}_{\mathrm{sc}}\times\mathbf{H}_{\mathrm{sc}}^*])_r \\ &= \frac{c\lambda}{(16\pi^2)}\Re\left\{i\psi_{\mathrm{sc}}\left(\frac{\partial\psi_{\mathrm{sc}}}{\partial r}\right)^*\right\}, \end{aligned} \tag{10}$$

where c is the speed of light in vacuum. We define the far field intensity scattered at the angle θ as an amount proportional to $(\mathbf{S}_{\mathrm{sc}})_r$:

$$\text{Intensity} \sim (\mathbf{S}_{\mathrm{sc}})_r. \tag{11}$$

The numerical solution of Eq. (6) requires a discretization procedure, i.e., the continuous parameter t is replaced by a set of N elements $[t_1, \ldots, t_N]$. Therefore, Eq. (6) becomes a matrix equation:

$$\psi(t_m) = \psi_{\mathrm{inc}}(t_m) + \sum_{n=1}^{n=N} H_{mn}\psi(t_n). \tag{12}$$

The matrix elements H_{mn} can be written as [23]

where $\Delta t_n = t_n - t_{n-1}$ is the length of the sampling intervals, $\xi_m' = [\mathrm{d}\xi/\mathrm{d}t](t_m)$, $\xi_m'' = [\mathrm{d}^2\xi/\mathrm{d}t^2](t_m)$, $\eta_m' = [\mathrm{d}\xi/\mathrm{d}t](t_m)$, $\eta_m'' = [\mathrm{d}^2\xi/\mathrm{d}t^2](t_m)$, $u_{mn} = \xi_m - \xi_n$, and $w_{mn} = \eta_m - \eta_n$.

Numerical tests were initially performed with the profile shown in Fig. 1(c). The abrupt change of this profile (and of its normal derivative) at points A and B produces numerical instabilities that make it difficult to achieve convergence of the results. For instance, in certain wavelength ranges the field intensity shows significant variations when the parameter N is slightly changed. To overcome this problem, the hard edges of the cavities were rounded as shown in Fig. 1(d). In contrast with the geometry of Fig. 1(c), numerical tests with the profile of Fig. 1(d) showed very good convergence of the results as a function of the parameter N. The curves presented in the next section were obtained by taking $N \approx 1300$.

3. Results

When the incident wavelength considerably exceeds the dimensions of the structure, phase resonances can be excited [20]. Our purpose is to investigate the phase resonances that appear in a perfectly conducting surface with a finite number of cylindrical grooves, their properties, and their dependence with the geometrical parameters. In Fig. 2 we analyze the dependence of the resonances on the number of

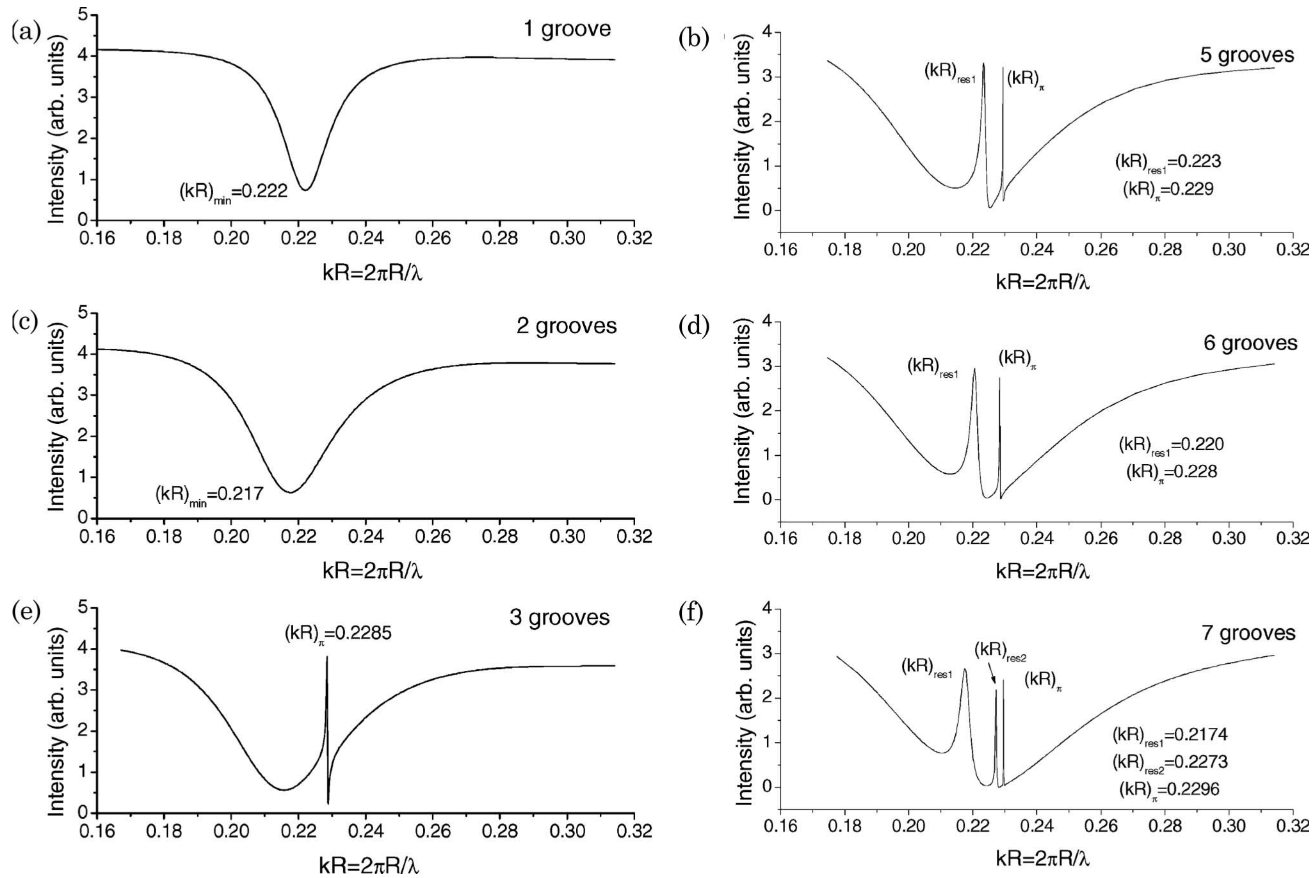

Fig. 2. Reflected intensity as a function of kR for a p-polarized Gaussian beam of width $W = 20R$ normally incident on a finite grating with an aperture $a/R = 0.02826$; the distance between adjacent grooves is $d = 2.1R$. (a) $N = 1$, (b) $N = 2$, (c) $N = 3$, (d) $N = 5$, (e) $N = 6$, (f) $N = 7$.

grooves. We consider grooves of circular cross section with an aperture $a/R = 0.02826$, separated a distance $d = 2.1R$, and study the specularly reflected response for a normally incident p-polarized Gaussian beam of spatial width $W = 20R$ as a function of kR. In the range of kR considered, the curves for one and two grooves exhibit a minimum, which is associated with the so called H_{00} mode [26] [see Figs. 2(a) and 2(b)]. From the mathematical point of view, this low-frequency resonance has a singular nature. The eigenmodes of a perfectly conducting waveguide with circular cross section for p polarization include the zero as its lowest eigenfrequency, but since its associated eigenfunction is identically equal to zero, this is not a true eigenvalue. The effect of cutting the cylinder and making an aperture is to shift this zero pseudo-eigenvalue by a small complex number with a corresponding nonzero eigenfunction. In terms of an equivalent circuit, the aperture causes a break in the transverse current on the cylinder, which results in an equivalent capacitance and inductance that produce the resonance [27]. The frequency at which this resonance occurs increases with the aperture size [28], and in this case is found approximately at $kR = 0.22$. Although the minimum in the reflected response associated to the H_{00} mode stays for an arbitrary number of grooves, a sharp peak appears in the reflected response for the three-groove case at $kR = 0.2285$, as observed in Fig. 2(c). This peak corresponds to the so called π resonance, and arises from the resonant coupling of the electromagnetic field within adjacent grooves, as it was already observed for grooves of rectangular cross section [7]. For this particular wavelength, the field phases in adjacent grooves are opposite to each other, and this produces a reflectance maximum. In Fig. 3(a) we show the magnitude of the magnetic field at the center of each groove as a function of kR, for the case of three grooves considered in Fig. 2. In this figure, the labels L, C, and R correspond to left, central, and right grooves, respectively. A remarkable intensification of the interior field is obtained at the π resonance. The phase difference between the magnetic fields at the center of adjacent grooves is shown in Fig. 3(b). Notice that due to the symmetry imposed by the normal incidence, both external grooves have the same field, and then the phase difference between the right and the central groove is the same as that between the left and the central one. This phase difference curve confirms that the π resonance is associated with a phase difference of π radians between the magnetic fields at adjacent grooves. If we keep increasing the number of grooves in the surface, we obtain the curves in Figs. 2(d)–2(f): for five and six grooves there are two maxima within the same waveguide resonance minimum, and for

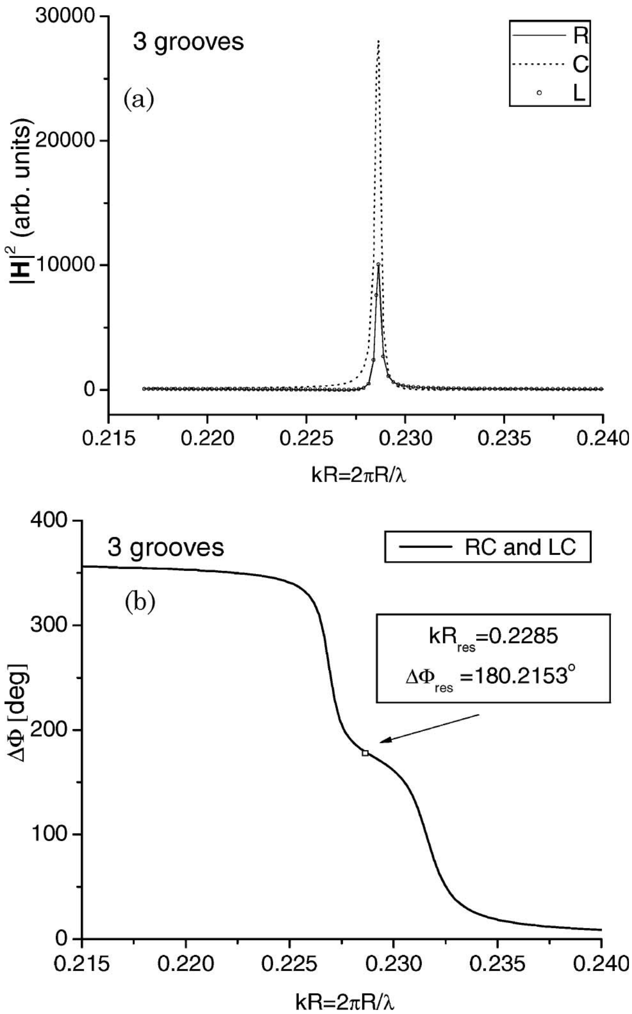

Fig. 3. Magnetic field at the center of each groove as a function of kR for the three-groove case considered in Fig. 2(c). (a) $|H|^2$, (b) phase difference between the external and the central grooves.

seven grooves, even one more peak appears. This trend is to be expected, and the same behavior was found in surfaces with rectangular grooves [7]. The appearance of more peaks is related to the increase in the number of possibilities to get opposite phases in adjacent grooves. In the case of three grooves under normal incidence, the only possibility is to have the same phase at the external grooves, opposite to the central one. Such a phase pattern is also denoted as (+-+) according to the terminology already used in the literature [7,12,17]. For five grooves, more phase configurations could be found, such as (+- + - +), (+- - - +), and (+ + - + +). The highest quality peak corresponds to the π resonance (opposite phases in any pair of adjacent grooves), whereas for the other modes the quality slightly decreases. In all cases, the π resonance is located at the largest value of kR among all the phase resonance modes, as observed in the rectangular grooves case [7]. It is interesting to notice that in the case of six grooves, there are also two peaks as in the five-groove case, but the resonances have less quality. This occurs since, even though in the six-groove case there are also three possibilities of phase distributions, namely, (+- + +- +), (+ + - - + +), and (+ - - - - +), none of them has opposite phases in every pair of adjacent grooves, as required for the π resonance, since this situation is forbidden due to the symmetry imposed by the normally incident plane wave.

The amplitude and phase of the magnetic interior field for the five-groove case is shown in Fig. 4. In these figures, the labels LL and RR correspond to leftmost and rightmost grooves, respectively, the L and R labels correspond to the grooves at the left and right of the central one, respectively, and C corresponds to the central groove. According to Figs. 4(d) and 4(e), the resonance at $kR \approx 0.229$ corresponds to the π mode (+- + - +), and that at $kR \approx 0.223$ corresponds to the mode (+- - - +). It can be observed in Figs. 4(a)–4(c) that the field within all the grooves is significantly enhanced at the π resonance, and at the other mode the field is intensified in the external and the central grooves only. This is a characteristic of phase resonances, as previously observed for other systems [7,20].

When the incidence is no longer normal, new phase configurations are allowed, and then more resonant peaks may appear in the reflected response. An example of this is shown in Fig. 5, where we show the reflected intensity and the phase and magnitude of the magnetic field within the rulings for a two-groove structure with the same parameters considered in Fig. 2, and for oblique incidence, $\theta_0 = 40°$. A resonant peak that was not present in the normal incidence case (included in this figure for comparison) appears, and, as can be learned from Fig. 5(b), it roughly corresponds to a (+ -) mode, which is a forbidden mode for normal incidence due to symmetry reasons. At this resonance, the magnetic field within both grooves is significantly enhanced, as observed in Figs. 5(c) and 5(d) (the reflected response for the same structure under normal illumination is also included for comparison).

In Fig. 6 we analyze the influence of the aperture size on the reflected response, and, in particular, on the π resonance for the three-groove case. Four values of the aperture have been considered, and the corresponding intensity curves are shown in Fig. 6(a). It can be observed that as the aperture decreases, the resonant value of kR also decreases, as is expected for the H_{00} mode in a slotted cylinder [28]. A shift in the resonant frequencies of an open cavity when varying its aperture size is a general characteristic of cavity resonances; the case of bottle-shaped cavities was investigated in [29,30]. As the aperture decreases, the resonances become more localized, and their widths also decrease. The possibility of tuning the frequency by varying the aperture size is an interesting characteristic of phase resonances, which suggests that these systems could be used as frequency selective devices. The resonant frequency as a function of the normalized aperture size is shown in Fig. 6(b). This curve shows that for variations of the

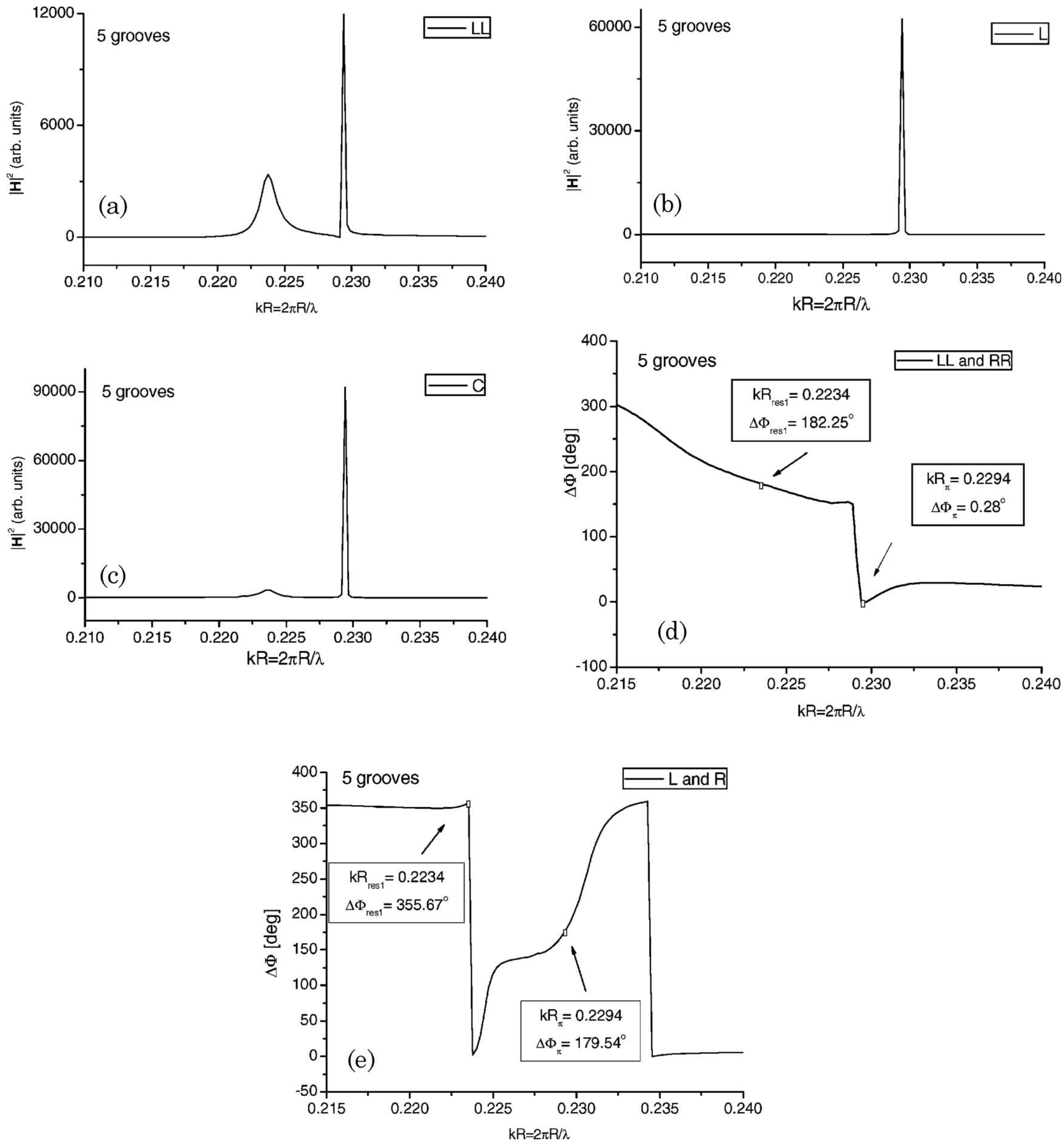

Fig. 4. Magnetic field at the center of each groove as a function of kR for the five-groove case considered in Fig. 2(d). (a) $|H|^2$ in the leftmost groove, (b) $|H|^2$ in the second groove, (c) $|H|^2$ in the central groove, (d) phase difference between the leftmost and the central groove, (e) phase difference between the second and the central groove.

aperture size within 10% of the radius R, the resonant kR varies significantly, and this confirms the tunability of the system.

In Fig. 7 we analyze a structure comprising six grooves, forming two subsets of three grooves each, separated a distance $D = d + \Delta$. We show the reflected intensity as a function of kR for different ratios Δ/R between 0 and 6. For $\Delta/R = 0$, the structure is the regular six-groove surface already considered in Fig. 2(e), in which all the grooves are equally spaced. Its response is represented by the thick solid line in Fig. 7, where two phase resonances are identified: the highest quality resonance at $kR = 0.228$, which in the six-groove case corresponds to the (+- + + - +) mode, and the (+ + - - + +) mode at $kR = 0.22$. As the distance between both three-groove groups is increased, the π resonance peak is present in all the reflected spectra, whereas the leftmost resonance peak weakens, and for $\Delta/R = 6$ almost vanishes. This behavior can be explained in terms of the electromagnetic coupling between adjacent grooves. When the grooves are equally spaced, several possibilities of exciting phase resonances are allowed, as discussed above in connection to Fig. 2. However, as Δ increases, the coupling between both central grooves becomes weaker, and in the limit of very large Δ the system behaves like two noninteracting subsets of three grooves. Thus only the modes corresponding to each one of the three-groove subsets can be excited, which in the normal incidence

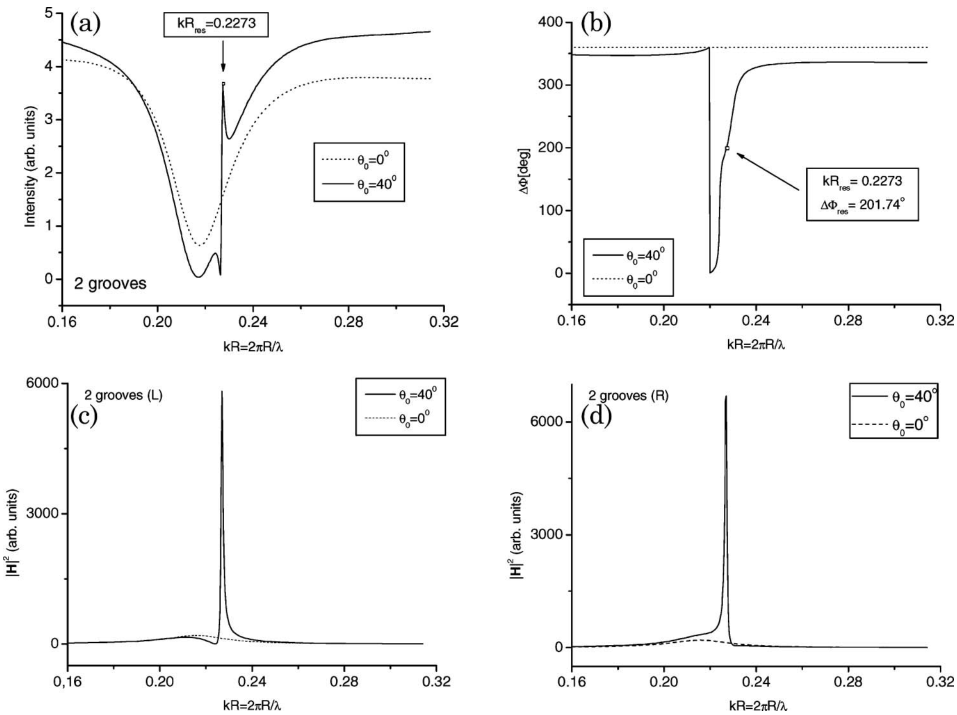

Fig. 5. (a) Reflected intensity as a function of kR for a p-polarized Gaussian beam of width $W = 20R$, incident with an angle $\theta_0 = 40°$, on a two-groove grating with an aperture $a/R = 0.02826$ and distance between grooves of $d = 2.1R$; (b) phase difference between the magnetic field at the center of each groove in the same case; (c) $|\mathrm{H}|^2$ at the center of the left groove; (d) $|\mathrm{H}|^2$ at the center of the right groove.

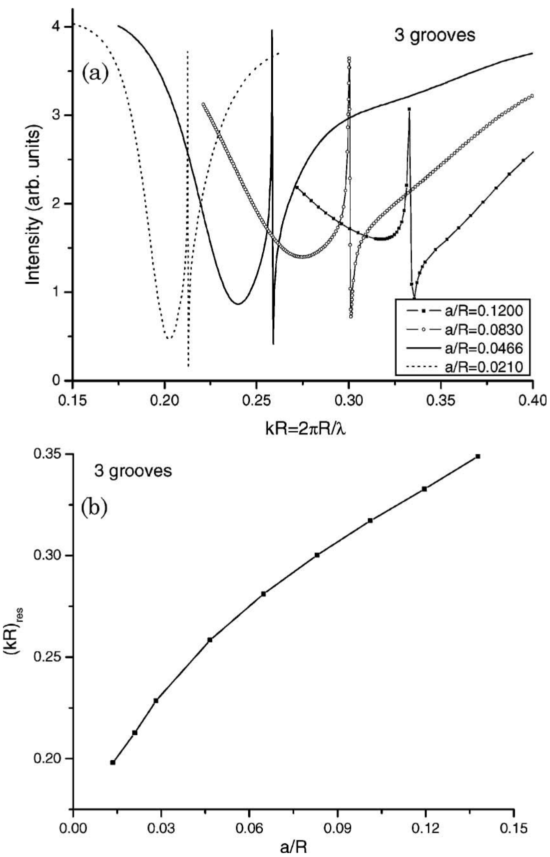

Fig. 6. Dependence of the resonant kR value on the aperture size for the three-groove case considered in the previous figures. (a) Reflected intensity as a function of kR for several values of the aperture; (b) resonant kR as a function of the normalized aperture size.

case is only the (+ - +) mode, represented by the narrow peak at $kR = 0.228$. The response of a structure with just three equally spaced grooves is also included for comparison (circles), where it is evident that only the π resonance is present.

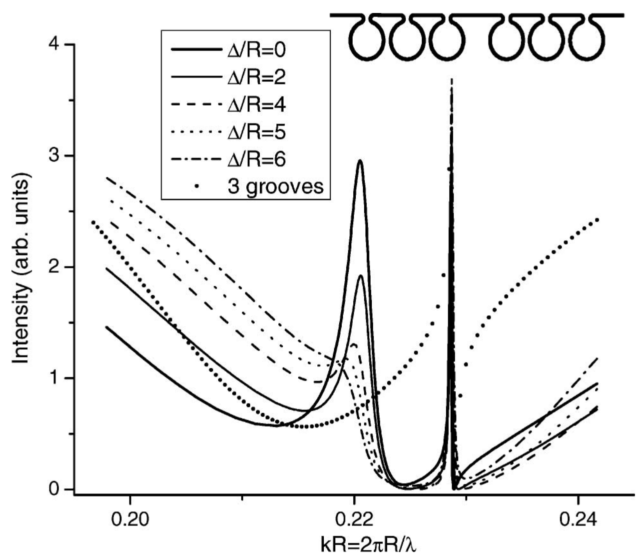

Fig. 7. Reflected intensity as a function of kR for a p-polarized Gaussian beam of width $W = 20R$, normally incident on a structure comprising six grooves, forming two subsets of three grooves of aperture $a/R = 0.02826$ and $d = 2.1R$ each, separated a distance $D = d + \Delta$. The different curves correspond to different ratios Δ/R.

4. Conclusions

We have investigated the electromagnetic response of finite arrays of subwavelength grooves of circular cross section, and found that phase resonances can be excited for particular wavelengths. The integral method has been developed and applied to solve the scattering problem, and special attention was paid to the treatment of sharp boundaries. The excitation of phase resonances in this system has been studied, and the dependence of their spectral location with the number of grooves and with the aperture size has been analyzed for potential applications such as frequency selectors and polarizers. The magnetic field within the grooves was also calculated, and the results confirm that phase resonances are characterized by a significant enhancement of the interior field. This work constitutes the first study of phase resonances in finite gratings with nonrectangular geometry.

The authors gratefully acknowledge partial support from Consejo Nacional de Investigaciones Científicas y Técnicas (CONICET), Universidad de Buenos Aires (UBA), Agencia Nacional de Promoción Científica y Tecnológica (ANPCYT-BID 1728/OC-AR06-01785), and Programa de Movilidad Académica de la Universidad Autónoma de Baja California (UABC), 6ta Convocatoria.

References

1. E. Goulielmakis, G. Nersisyan, N. Papadogiannis, D. Charalambidis, G. Tsakiris, and K. Witte, "A dispersionless Michelson interferometer for the characterization of attosecond pulses," Appl. Phys. B **74**, 197–206 (2002).
2. J. J. Wang, F. Liu, X. Deng, X. Liu, L. Chen, P. Sciortino, and R. Varghese, "Monolithically integrated circular polarizers with two-layer nano-gratings fabricated by imprint lithography," J. Vac. Sci. Technol. B **23**, 3164–3167 (2005).
3. T. W. Ebbesen, H. J. Lezec, H. F. Ghaemi, T. Thio, and P. A. Wolff, "Extraordinary optical transmission through sub-wavelength hole arrays," Nature **391**, 667–669 (1998).
4. H. F. Ghaemi, T. Thio, D. E. Grupp, T. W. Ebbesen, and H. J. Lezec, "Surface plasmons enhance optical transmission through subwavelength holes," Phys. Rev. B **58**, 6779–6782 (1998).
5. J. A. Porto, F. J. García-Vidal, and J. B. Pendry, "Transmission resonances on metallic gratings with very narrow slits," Phys. Rev. Lett. **83**, 2845–2848 (1999).
6. F. J. García-Vidal and L. Martín-Moreno, "Transmission and focusing of light in one-dimensional periodically nanostructures metals," Phys. Rev. B **66**, 155412 (2002).
7. D. C. Skigin, V. V. Veremey, and R. Mittra, "Superdirective radiation from finite gratings of rectangular grooves," IEEE Trans. Antennas Propag. **47**, 376–383 (1999).
8. A. N. Fantino, S. I. Grosz, and D. C. Skigin, "Resonant effect in periodic gratings comprising a finite number of grooves in each period," Phys. Rev. E **64**, 016605 (2001).
9. S. I. Grosz, D. C. Skigin, and A. N. Fantino, "Resonant effects in compound diffraction gratings: influence of the geometrical parameters of the surface," Phys. Rev. E **65**, 056619 (2002).
10. D. C. Skigin, A. N. Fantino, and S. I. Grosz, "Phase resonances in compound metallic gratings," J. Opt. A Pure Appl. Opt. **5**, S129–S135 (2003).
11. J. Le Perchec, P. Quemerais, A. Barbara, and T. Lopez-Rıos, "Controlling strong electromagnetic fields at subwavelength scales," Phys. Rev. Lett. **97**, 036405 (2006).
12. D. C. Skigin and R. A. Depine, "Transmission resonances on metallic compound gratings with subwavelength slits," Phys. Rev. Lett. **95**, 217402 (2005).
13. D. C. Skigin and R. A. Depine, "Resonances on metallic compound transmission gratings with subwavelength wires and slits," Opt. Commun. **262**, 270–275 (2006).
14. D. C. Skigin and R. A. Depine, "Narrow gaps for transmission through metallic structured gratings with subwavelength slits," Phys. Rev. E **74**, 046606 (2006).
15. A. P. Hibbins I. R. Hooper, M. J. Lockyear, and J. R. Sambles, "Microwave transmission of a compound metal grating," Phys. Rev. Lett. **96**, 257402 (2006).
16. D. C. Skigin, H. Loui, Z. Popovic, and E. Kuester, "Bandwidth control of forbidden transmission gaps in compound structures with subwavelength slits," Phys. Rev. E **76**, 016604 (2007).
17. Y. G. Ma, X. S. Rao, G. F. Zhang, and C. K. Ong, "Microwave transmission modes in compound metallic gratings," Phys. Rev. B **76**, 085413 (2007).
18. A. Barbara, J. Le Perchec, S. Collin, C. Sauvan, J.-L. Pelouard, T. López-Ríos, and P. Quémerais, "Generation and control of hot spots on commensurate metallic gratings," Opt. Express **16**, 19127–19135 (2008).
19. M. Navarro-Cía, D. C. Skigin, M. Beruete, and M. Sorolla, "Experimental demonstration of phase resonances in metallic compound gratings with subwavelength slits in the millimeter wave regime," Appl. Phys. Lett. **94**, 091107 (2009).
20. V. V. Veremey and R. Mittra, "Scattering from structures formed by resonant elements," IEEE Trans. Antennas Propag. **46**, 494–501 (1998).
21. A. A. Maradudin, T. Michel, A. R. McGurn, and E. R. Méndez, "Enhanced backscattering of light from a random grating," Ann. Phys. (N.Y.) **203**, 255–307 (1990).
22. C. I. Valencia and R. A. Depine, "Resonant scattering of light by an open cylindrical cavity ruled on a highly conducting flat surfaces," Opt. Commun. **159**, 254–265 (1999).
23. C. I. Valencia, E. R. Méndez, and B. S. Mendoza, "Second harmonic generation in the scattering of light by two dimensional particles," J. Opt. Soc. Am. B **20**, 2150–2161 (2003).
24. R. Goloskie, T. Thio, and L. R. Ram-Mohan, "Boundary elements and surface plasmons," Comput. Phys. **10**, 477–495 (1996).
25. M. Abramowitz and I. A. Stegun, *Handbook of Mathematical Functions* (Dover, 1970), p. 364.
26. D. Colak, A. I. Nosich, and A. Altintas, "Radar cross-section study of cylindrical cavity-backed apertures with outer or inner material coating: the case of H-polarization," IEEE Trans. Antennas Propag. **43**, 440–447 (1995).
27. R. W. Ziolkowski and J. B. Grant, "Scattering from cavity-backed apertures: the generalized dual series solution of the concentrically loaded E-pol slit cylinder problem," IEEE Trans. Antennas Propag. **35**, 504–528 (1987).
28. P. M. Goggans and T. H. Shumpert, "Backscatter RCS for TE and TM excitations of dielectric-filled cavity-backed apertures in two-dimensional bodies," IEEE Trans. Antennas Propag. **39**, 1224–1227 (1991).
29. D. C. Skigin and R. A. Depine, "Resonant enhancement of the field within a single ground-plane cavity: comparison of different rectangular shapes," Phys. Rev. E **59**, 3661–3668 (1999).
30. D. C. Skigin and R. A. Depine, "Resonant modes of a bottle-shaped cavity and their effects in the response of finite and infinite gratings," Phys. Rev. E **61**, 4479–4490 (2000).